

Full paper / Mémoire

Synthesis of unsupported Ni–W–S hydrotreating catalysts from the oxothiosalt $(\text{NH}_4)_2\text{WO}_2\text{S}_2$

Zhang Le ^a, Pavel Afanasiev ^{b,*}, Dadong Li ^a, Yahua Shi ^a, Michel Vrinat ^a

^a *Research Institute of Petroleum Processing, SINOPEC, 18 Xue Yuan Road, 100083 Beijing, PR China*

^b *Institut de recherches sur la catalyse et l'environnement, 2, avenue Albert-Einstein, 69626 Villeurbanne cedex, France*

Received 16 January 2007; accepted after revision 24 April 2007

Available online 19 June 2007

Abstract

Synthetic routes for the preparation of unsupported Ni–W–S hydrotreating catalysts were studied. In the preparations studied, amorphous tungsten oxysulfide WO_xS_y was used obtained from the acid condensation or thermal decomposition of $(\text{NH}_4)_2\text{WO}_2\text{S}_2$ salt. Amorphous WO_xS_y solid was promoted by nickel salt solutions and eventually stabilized by addition of organic molecules. The products were characterized by X-ray powder diffraction, specific surface area and pore volume measurements. The catalytic activities of Ni–W–S systems were evaluated for the thiophene hydrodesulfurization (HDS) reaction. It has been shown that highly active unsupported tungsten sulfides can be obtained from thermal decomposition of $(\text{NH}_4)_2\text{WO}_2\text{S}_2$ but not from acid condensation. Addition of organics such as nonionic Triton 114 surfactant to the impregnating solution strongly improved the textural properties and HDS activity of the unsupported Ni–W–S catalysts. **To cite this article:** Z. Le et al., *C. R. Chimie 11 (2008)*.

© 2007 Académie des sciences. Published by Elsevier Masson SAS. All rights reserved.

Résumé

Des voies de synthèse pour la préparation de catalyseurs massiques Ni–W–S de l'hydrotraitement ont été étudiées. Dans les préparations étudiées, l'oxysulfure amorphe WO_xS_y de tungstène, obtenu à partir de la condensation acide ou de la décomposition thermique du sel $(\text{NH}_4)_2\text{WO}_2\text{S}_2$, a été utilisé. Le solide amorphe WO_xS_y a été ensuite promu par des solutions de sels de nickel et stabilisé par l'addition de molécules organiques. Les produits ont été caractérisés par diffraction sur poudre (DRX) ainsi que par des mesures de surfaces spécifiques et de volumes de pores. Les activités catalytiques des systèmes Ni–W–S ont été évaluées pour la réaction d'hydrodésulfuration de thiophène (HDS). Nous avons montré que des catalyseurs non supportés très actifs de sulfure de tungstène peuvent être obtenus par décomposition thermique de $(\text{NH}_4)_2\text{WO}_2\text{S}_2$, mais pas par condensation acide. L'addition de produits organiques tels que l'éthylène glycol et l'agent tensioactif non ionique Triton 114 à la solution d'imprégnation ont fortement amélioré les propriétés de texture et l'activité HDS des catalyseurs Ni–W–S. **Pour citer cet article :** Z. Le et al., *C. R. Chimie 11 (2008)*.

© 2007 Académie des sciences. Published by Elsevier Masson SAS. All rights reserved.

Keywords: Nickel; Tungsten; Unsupported catalyst; Hydrotreating; Thiosalt; Surfactant

Mots-clés : Nickel ; Tungstène ; Catalyseur non supporté ; Hydrotraitement ; Thiosel ; Agent tensioactif

* Corresponding author.

E-mail address: afanas@catalyse.univ-lyon1.fr (P. Afanasiev).

1. Introduction

The hydrotreatment of petroleum aims to produce clean gasoline and diesel with low sulfur, nitrogen and aromatics contents. More stringent environmental regulations require increase of the efficiency of these processes. Among the possible solutions, using more active catalysts would be less expensive for the refineries, because it would allow avoiding modifications for the plant installations.

Conventional HDS catalysts contain molybdenum sulfide MoS_2 (10–20 wt%) promoted with cobalt or nickel (3–5 wt%) and supported on alumina. Recently, new types of catalysts appeared, which contain very high amount of MoS_2 and can be considered as unsupported systems. Development of such unsupported systems possessing advantageous textural properties and bearing very high density of active sites seems to be a promising research direction.

Earlier, unsupported hydrotreating catalysts have been prepared by different methods, including comaceration [1], homogenous sulfide precipitation [2–6], thio-salt decomposition [7–9], hydrothermal and solvothermal processes [10–14], and solution reactions [15,16]. Thus prepared molybdenum sulfide can be further promoted by cobalt or nickel [17–19].

Thiometallates are used for many applications spreading from biological systems [20–23] to catalyst precursors [7–9,24–29]. Several works have reported the use of thiometallates to generate MoS_2 and WS_2 catalysts with high surface area and high catalytic activity [30–32].

The goal of this work was to prepare highly active unsupported Ni–W sulfides, which actually are somewhat less studied than the molybdenum counterparts. In this study, unsupported Ni–W–S catalysts were prepared using ammonium oxothio tungstate $(\text{NH}_4)_2\text{WO}_2\text{S}_2$ as precursor.

2. Experimental

2.1. Preparation of W oxothiosalt precursor

The precursor $(\text{NH}_4)_2\text{WO}_2\text{S}_2$ was prepared by ammonium sulfide precipitation as follows. Ammonium metatungstate (20 g, ca 0.1 mol W) was dissolved in 50 mL of concentrated NH_4OH and 40 mL H_2O . The mixture was stirred for 1 h (to depolymerize polytungstate species to get monomeric WO_4^{2-} , which can be a slow process). Then 100 mL of $(\text{NH}_4)_2\text{S}$ (50 wt%) were rapidly added to the solution at ambient temperature. The yellow precipitate was recovered by filtration

and dried under nitrogen flow at room temperature. It was identified by XRD and chemical analysis.

2.2. Preparation of Ni–W–S catalysts

Amorphous W oxysulfide pre-catalysts WO_xS_y were prepared either by solution acid condensation of $\text{WO}_2\text{S}_2^{2-}$ anions (protonation followed by water splitting) or by thermal decomposition of the $(\text{NH}_4)_2\text{WO}_2\text{S}_2$ salt at different temperatures (heating rate: 4 °C/min). The oxysulfide amorphous solids were kept and handled under nitrogen. To prepare the Ni–W–S catalysts, the oxysulfide solids were impregnated with appropriate amounts of aqueous $\text{Ni}(\text{NO}_3)_2$, eventually in the presence of ethylene glycol and/or polyethylene oxide-based organic surfactant Triton 114 (50 vol% ethylene glycol, 15% surfactant). The technique applied and the molar quantities of the reactants were similar to those used earlier for molybdenum [33,34]. The black solids after nickel impregnation were sulfided under 15 vol% of $\text{H}_2\text{S}/\text{H}_2$ at 400 °C for 4 h.

2.3. Characterizations

The X-ray diffraction patterns were obtained on a BRUKER diffractometer with the $\text{Cu K}\alpha$ radiation. Standard JCPDS files were employed to identify the present phases. Chemical analyses were performed using the atomic emission method with a spectroflame ICPD device. The surface areas and pore volumes were determined by nitrogen adsorption at 77 K using, respectively, the BET and the BJH equations. High-resolution transmission electron microscopy (HREM) and energy-dispersive X-ray analysis (EDX) were done on a JEOL 2010 device.

2.4. Catalytic test

Thiophene hydrodesulfurization (HDS) was carried out in the vapor phase in a fixed microreactor operated in the dynamic mode at atmospheric pressure of hydrogen (thiophene pressure: 2.4 kPa, obtained by saturation at 0 °C; total mass flow: 6 L/h). A catalyst charge of about 0.07 g was employed. The reaction rate was measured at 340 °C in steady-state conditions after 16 h of stream. The reaction products were analyzed chromatographically, using an online gas chromatograph HP5890 equipped with a flame ionization detector and a 30 m × 0.53 mm capillary column. The PLOT (Porous Layer Open Tubular) column is a fused silica capillary column coated with a homogenous layer of particles of Al_2O_3 deactivated by Na_2SO_4 . The analysis

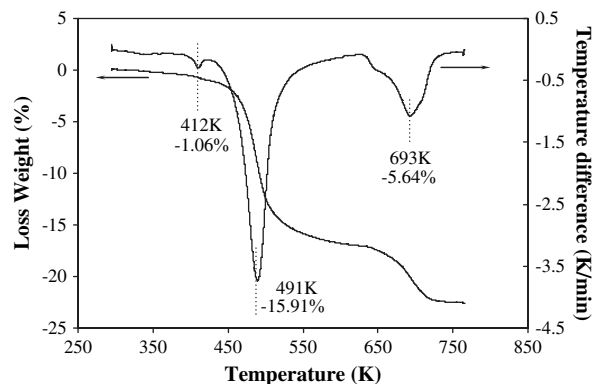


Fig. 1. DTA–TGA curve of the decomposition of ammonium oxothiotungstate precursor.

was performed with a temperature program: 80 °C for 1 min, then heating to 190 °C at 20 °C/min and dwell at 190 °C for 28 min.

3. Results and discussion

3.1. Synthesis and characterization of the WOS_2 precursor

Earlier, we described solution preparations of highly loaded or unsupported Mo-based catalysts [33,34]. Thiooxomolybdate $(NH_4)_2MoO_2S_2$ was successfully used in Ref. [33] to prepare at first high-surface-area $MoOS_2$ amorphous oxosulfide, then to promote it with cobalt. In this work, we used a $(NH_4)_2WO_2S_2$ salt because it is much easier to prepare than completely sulfided thiotungstates such as WS_4^{2-} salts. The $(NH_4)_2WO_2S_2$ salt can be obtained at ambient conditions by addition of aqueous ammonium sulfide to the metatungstate solution, whereas the thiotungstate preparation requires H_2S bubbling through a solution with thorough control of temperature. At the same time the oxothiotungstate contains two sulfur atoms per tungsten, hopefully sufficient to produce WS_2 with the following reactions.

Table 1

Evolution of W and S contents in the solids obtained by decomposition of ammonium oxothiotungstate

| Solid | Heating temperature (°C) | W (wt%) | S (wt%) | S/W (mol) |
|---------------------------|--------------------------|---------|---------|-----------|
| Initial $(NH_4)_2WO_2S_2$ | RT | 57.54 | 20.25 | 2.02 |
| W-n-150 | 150 | 58.88 | 22.68 | 2.21 |
| W-hs-150 | 150 | 58.18 | 23.86 | 2.35 |
| W-hs-200 | 200 | 62.03 | 26.96 | 2.49 |
| W-hs-400 | 400 | 66.81 | 21.16 | 1.82 |

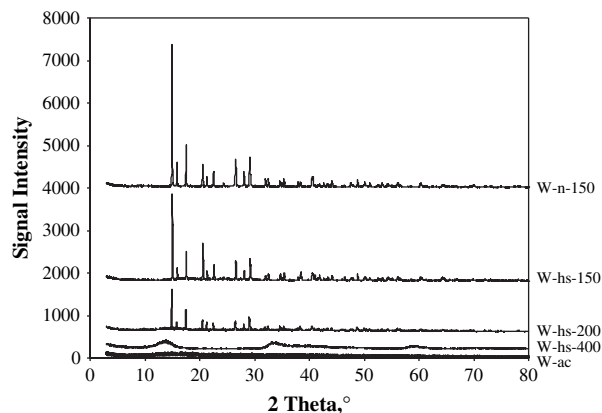
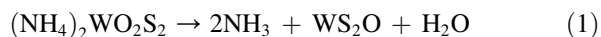


Fig. 2. XRD patterns of tungsten solid prepared with different conditions. The intense diffraction lines are all those of $(NH_4)_2WO_2S_2$ phase, broad peaks – WS_2 phase.

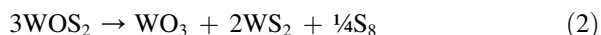
In the proposed method, we first obtained a high-surface-area amorphous solid by decomposition of the crystalline precursor, then promoted this solid with nickel, and further reactivated it. The decomposition step is therefore of primary importance.

The DTA–TGA analyses were used to characterize the thermal decomposition of ammonium oxothiotungstate. From thermal decomposition curves (Fig. 1), three endothermic peaks could be clearly distinguished, and the total mass loss was 22.60% (from ambient temperature to 763 K). Small weight loss (1.06%) was observed at low temperature (412 K), and may be attributed to the elimination of absorbed water. The second step of decomposition occurred in the 423–613 K temperature range with an endothermic peak, and is supposed to be due to the reaction (1):



According to this equation, the decomposition of tungsten oxosulfide should have a theoretical weight loss of 16.47%, which is close to the observed value of the step with a mass loss of 15.91%.

The third decomposition step occurred from 613 to 763 K with a weight loss of 5.64%. No further mass loss was observed under nitrogen flow. According to the XRD pattern (not shown), the product after the decomposition at temperatures as high as 973 K contained WO_3 and WS_2 phases. It might therefore be related to the rearrangement of the amorphous tungsten oxosulfide structure to crystalline phases with partial expulsion of sulfur according to reaction (2):



with a theoretical weight loss of 6.7%.

Table 2
Properties of the Ni–W–S catalysts as a function of preparation mode

| Catalysts | Pre-catalyst | Solvent for nickel salt | R | S (wt%) | C (wt%) | S (m ² /g) | V (cm ³ /g) | HDS rate (10 ⁻⁸ mol/(g s)) | | |
|------------------------------------|------------------------------------|-------------------------|------|---------|---------|-----------------------|------------------------|---------------------------------------|-------|-------|
| | | | | | | | | 573 K | 593 K | 613 K |
| NiW/Al ₂ O ₃ | NiW/Al ₂ O ₃ | Reference | | | | | | 187 | 285 | 434 |
| NiW-ac | W-ac | H ₂ O | 0.5 | 30.19 | 1.75 | 0.52 | – | 13 | 24 | 39 |
| NiW-n | W-n | H ₂ O | | 35.99 | 1.26 | 29.0 | 0.11 | 31 | 40 | 45 |
| NiW-ne | W-n | H ₂ O + EG | | 38.59 | 2.98 | 19.27 | 0.06 | 116 | 170 | 205 |
| NiW-hs150e | W-hs-150 | H ₂ O + EG | 0.43 | 39.43 | 1.51 | 23.7 | 0.06 | 125 | 243 | 415 |
| NiW-hs200e | W-hs-200 | H ₂ O + EG | 0.33 | 33.48 | 1.66 | 16.21 | 0.05 | 118 | 224 | 374 |
| NiW-hs400e | W-hs-400 | H ₂ O + EG | 0.35 | 34.34 | 2.48 | 6.25 | – | 6 | 9 | 14 |

R = Ni/(Ni + W): mole ratio in the sulfide solid; W-n: solids obtained by means of heating in nitrogen; W-hs: solids obtained by means of heating under H₂S/H₂ flow; EG: ethylene glycol.

Alternative to the thermal decomposition, the oxysulfide solid was synthesized by acid condensation of a (NH₄)₂WO₂S₂ solution. Using this method, the yield of the solid product with respect to tungsten input was low (only 17%), and the properties of the oxysulfide solid were not very good (Table 2), so the decomposition by heating in an inert gas such as N₂ or 15 vol% H₂S/H₂ was further preferred. In the last case, we could not carry out the DTA–TGA analysis, but analyzed the composition and XRD patterns of solids after heating at different temperatures. The chemical compositions of tungsten oxosulfide products are shown in Table 1. Their diffraction patterns are shown in Fig. 2.

Chemical analysis shows that under H₂S/H₂ flow the S to W ratio increases slightly up to the temperature of the second peak of mass loss (but note that this temperature was measured under nitrogen flow). Apparently it happened due to some sulfidation of the W oxospecies by hydrogen sulphide. Then at 400 °C the S-to-W ratio drops, due to sulfur release. XRD patterns confirm progressive decrease of the intensity of sharp initial salt peaks. They are present even after 200 °C heating. Probably, the remaining oxothiosalt is located in the solid particles core and the products form amorphous exterior shell. The decomposition under hydrogen sulphide is therefore smooth and allows gentle control of the solids' properties.

After 400 °C the peaks of XRD reflections are very broad and approximately correspond to tungsten sulphide WS₂ (Fig. 2). The chemical composition of this

solid is, however, sulfur deficient compared to WS₂ stoichiometry, due to the presence of some oxide formed by the reaction (2).

3.2. Properties of the Ni-promoted catalysts

The solids heated at different temperatures were thereafter impregnated with nickel nitrate, then dried and re-sulfided at 400 °C and tested in thiophene HDS. The properties and activities of the catalysts prepared are shown in Table 2. In this table, the catalysts (NiW-xxx) designated in the first column were derived from the amorphous precursors (W-xxx) listed in the second column. The impregnation with nickel nitrate was carried out either in aqueous solution or in the mixture water–ethylene glycol (in the last case the NiW catalysts names contain the letter e at the end).

From Table 2 it follows that the as-prepared Ni–W–S catalysts had moderate specific surface areas and HDS activities, though their specific HDS performance was relatively high compared to the industrial reference NiW/Al₂O₃. Positive effect of ethylene glycol addition into the nickel nitrate impregnation solution can be clearly seen. Only the solids obtained by heating of the oxothiotungstate at 150–200 °C provided some reasonable activities. The W-ac preparation obtained by acid condensation and the W-hs400 solid obtained by heating at 400 °C both showed low surface areas and HDS performances. The X-ray diffraction patterns of the catalysts

Table 3
Comparison of the properties of the catalysts prepared using impregnation by Ni(NO₃)₂ dissolved in different solvents

| Catalysts | Solvent | R2 | C (wt%) | S (m ² /g) | V (cm ³ /g) | Rate (10 ⁻⁸ mol/(g s)) | | |
|------------------------------------|--------------------------------|------|---------|-----------------------|------------------------|-----------------------------------|-------|-------|
| | | | | | | 573 K | 593 K | 613 K |
| NiW/Al ₂ O ₃ | Reference | | 1.26 | 220 | | 187 | 285 | 434 |
| NiW-w | H ₂ O | | | 9 | 0.11 | 31 | 40 | 45 |
| NiW-we | H ₂ O + EG | 0.43 | 1.51 | 23.7 | 0.06 | 125 | 243 | 415 |
| NiW-wet | H ₂ O + EG + triton | 0.4 | 1.76 | 58.23 | 0.12 | 289 | 554 | 879 |

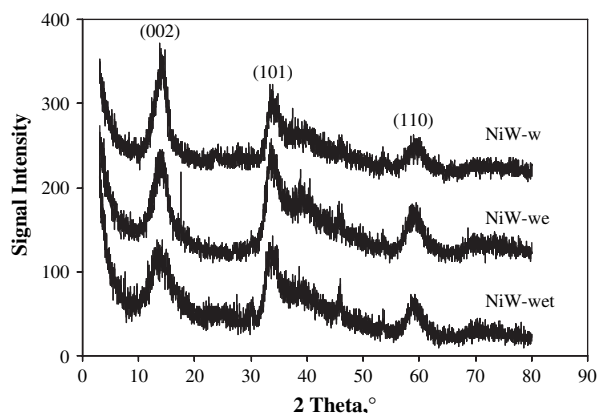


Fig. 3. XRD patterns of the Ni–W–S catalysts prepared with different solvents. All peaks correspond to the WS_2 phase.

listed in Table 2 were almost the same and they all showed only broad peaks of a tungsten disulfide compound.

Earlier we demonstrated for the MoS_2 -based catalysts [33,34] that the composition of the solvent plays a crucial role in the preparation of unsupported sulfide systems, since it determines the precursor's solubility, and also the parameters of nucleation and growth of the precipitate particles.

In the present work, we dealt with porous amorphous WO_xS_y solids insoluble in water or any organics. However, we impregnated them with the $\text{Ni}(\text{NO}_3)_2$ solutions containing the same type of organics as in Refs. [33,34]. It appeared that the influence of the impregnation solution's composition is strong and that qualitatively it has the same trend as was described for the precipitations. Indeed, only the addition of the nonionic surfactant Triton 114 allowed the obtaining a highly active system with increased specific surface area (Table 3).

From the diffraction patterns (Fig. 3), it seems that no great difference of WS_2 phase crystallinity was caused by the variations of the solvent. The intensity of the (002) peak at $2\theta = 14.3^\circ$, characteristic of the layer stacking along the c direction, decreased with the addition of EG and Triton. The stacking sizes calculated by line-broadening analysis were 2.97 nm (5 layers), 2.26 nm (4 layers) and 2.05 nm (3 layers), respectively, for the NiW-w, NiW-we and NiW-wet

catalysts. So, after organic compound and surfactant addition, the slabs in the NiW-wet sulfide catalyst became smaller and might be more divided. However, the differences observed in XRD are not very strong and do not explain the almost tenfold difference in the HDS activity.

Summarizing the influence of the impregnation solvent composition, it seems clear that it acts on the step of crystallization of WS_2 , improving its textural properties, but particularly it helps to optimize the Ni–W interaction. At the same time, the influence of mixed solvent on the precipitation step, as discussed earlier, [34] appears to be less important, since here we introduced the solutions into the porous amorphous solids and no precipitation occurred.

The properties of the unsupported catalysts may be further improved by adjusting the final activation (sulfidation) temperature (Table 4).

From Fig. 4, the specific surface area and thiophene HDS activity as a function of sulfiding temperature passed through a maximum at 450°C . Apparently, at the lower temperatures, the sulfidation was not complete, as it is known that tungsten species are rather difficult to transform to sulfide [35]. A maximum of the catalyst's surface area, pore volume, and thiophene HDS activity was observed at the middle 450°C sulfiding temperature. It might suggest that the NiW pre-catalyst was just totally sulfided at 450°C and temperatures higher than 450°C provoked sulfide sintering.

A high-resolution image of the optimized catalyst is represented in Fig. 5. We can see a porous structure constituted by the bent stacks of WS_2 slabs with approximate length 7–10 nm and the stacking degree of 3–5 slabs in each stack. No bulk NiS particles were observed by TEM in this specimen, suggesting good dispersion of nickel species, smeared over the tungsten sulfide.

4. Conclusion

A new technique has been developed in this work to obtain highly active Ni–W–S unsupported catalysts from the $(\text{NH}_4)_2\text{WO}_2\text{S}_2$ oxothiosalt. In this method, the parent salt was first decomposed to the state of

Table 4
Properties of the catalysts obtained using different sulfidation temperatures

| Catalysts | Sulfide temperature ($^\circ\text{C}$) | R1 | R2 | C (wt%) | S (m^2/g) | V (cm^3/g) | Rate (10^{-8} mol/(g s)) | | |
|------------------------------|--|------|-----|---------|-----------------------------|------------------------------|-----------------------------|-------|-------|
| | | | | | | | 573 K | 593 K | 613 K |
| NiW/ Al_2O_3 | Reference | | | | | | 187 | 285 | 434 |
| NiW-400 | 400 | 0.37 | 0.4 | 1.76 | 58.23 | 0.12 | 289 | 554 | 879 |
| NiW-450 | 450 | 0.37 | | 2.60 | 64.14 | 0.14 | 307 | 610 | 1038 |
| NiW-500 | 500 | 0.37 | | 1.15 | 46.69 | 0.11 | 180 | 358 | 623 |

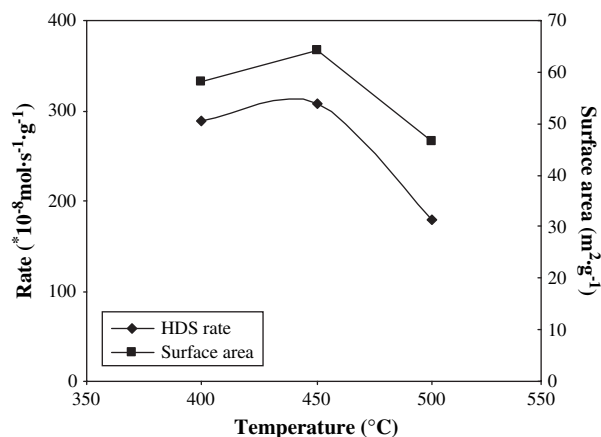


Fig. 4. Surface area and HDS rate as a function of sulfiding temperature.

amorphous oxosulfide and then the amorphous solid was impregnated with Ni salt. Conditions to obtain high specific surface area and HDS activity of the final sulfide solid were found. They include decomposition of the precursor salt at 150 °C and further impregnation with nickel salt dissolved in the ternary (water–

ethylene glycol nonionic surfactant) medium. Optimal sulfidation temperature was found to be 450 °C.

References

- [1] G. Hagenbach, P. Courty, B. Delmon, *J. Catal.* 31 (1973) 264.
- [2] R. Candia, B.S. Clausen, H. Topsøe, *J. Catal.* 77 (1982) 564.
- [3] R. Candia, B.S. Clausen, H. Topsøe, *Bull. Soc. Chim. Belg.* 90 (1981) 1225.
- [4] S. Göbböls, Q. Wu, F. Delannay, P. Grande, B. Delmon, J. Ladrière, *Polyhedron* 5 (1986) 219.
- [5] C. Gachet, R. Paulus, L. de Mourgues, C. Durand, H. Toulhoat, *Bull. Soc. Chim. Belg.* 93 (1984) 681.
- [6] F.B. Garreau, H. Toulhoat, S. Kasztelan, R. Paulus, *Polyhedron* 5 (1986) 211.
- [7] M. Zdražil, *Catal. Today* 3 (1988) 269.
- [8] S. Fuentes, G. Diaz, F. Pedraza, H. Rojas, N. Rosas, *J. Catal.* 113 (1988) 535.
- [9] U.S. Ozkan, L. Zhang, S. Ni, E. Moctezuma, *Energy Fuels* 8 (1994) 830.
- [10] Y.Y. Peng, Z.Y. Meng, C. Zhong, J. Lu, W.C. Yu, Z.P. Yang, Y.T. Qian, *J. Solid State Chem.* 159 (2001) 170.
- [11] Y.Y. Peng, Z.Y. Meng, C. Zhong, J. Lu, W.C. Yu, Z.P. Yang, Y.T. Qian, *Chem. Lett.* 30 (2001) 772.
- [12] W.J. Li, E.W. Shi, J.M. Ko, Z.Z. Chen, H. Ogino, T. Fukuda, *J. Cryst. Growth* 250 (2003) 418.
- [13] E. Devers, P. Afanasiev, B. Jouguet, M. Vrinat, *Catal. Lett.* 82 (2003) 13.
- [14] N. Rueda, R. Bacaud, M. Vrinat, *J. Catal.* 169 (1997) 404.
- [15] P. Afanasiev, G.F. Xia, G. Berhault, B. Jouguet, M. Lacroix, *Chem. Mater.* 11 (1999) 3216.
- [16] I. Bezverkhy, P. Afanasiev, M. Lacroix, *Inorg. Chem.* 39 (2000) 5416.
- [17] I. Bezverkhy, P. Afanasiev, C. Geantet, M. Lacroix, *J. Catal.* 204 (2001) 495.
- [18] I. Bezverkhy, P. Afanasiev, M. Lacroix, *J. Catal.* 230 (2005) 133.
- [19] Y. Ji, P. Afanasiev, M. Vrinat, W. Li, C. Li, *Appl. Catal., A* 257 (2004) 157.
- [20] S.P. Cramer, K.O. Hodgson, W.O. Gillum, L.E. Mortenson, *J. Am. Chem. Soc.* 100 (1978) 3398.
- [21] S.P. Cramer, W.O. Gillum, K.O. Hodgson, L.E. Mortenson, E.I. Stiefel, J.R. Chisnel, W.J. Brill, V.K. Shah, *J. Am. Chem. Soc.* 100 (1978) 3814.
- [22] A. Muller, E. Diemann, *Transition Metal Chemistry – Current Problems of General, Biological and Catalytical Relevances*, Verlag Chemie, Weinheim, Germany, 1981.
- [23] K.S. Liang, J. Bernholc, W.H. Pan, G.J. Hughes, E.I. Stiefel, *Inorg. Chem.* 26 (1987) 1422.
- [24] T.A. Pecoraro, R.R. Chianelli, U.S. Patent 4,528,089 to Exxon, 1985.
- [25] R.R. Chianelli, A.J. Jacobson, U.S. Patent 4,650,563 to Exxon, 1987.
- [26] A.W. Naumann, A.S. Behan, U.S. Patent 4,243,554 to Union Carbide, 1981.
- [27] T.C. Ho, W.H. Pan, U.S. Patent 4,514,517 to Exxon, 1985.
- [28] R.R. Chianelli, T.A. Pecoraro, U.S. Patent 4,508,847 to Exxon, 1985.
- [29] G. Alonso, G. Berhault, A. Aguilar, V. Cillins, C. Ornelas, S. Fuentes, R.R. Chianelli, *J. Catal.* 208 (2002) 359.

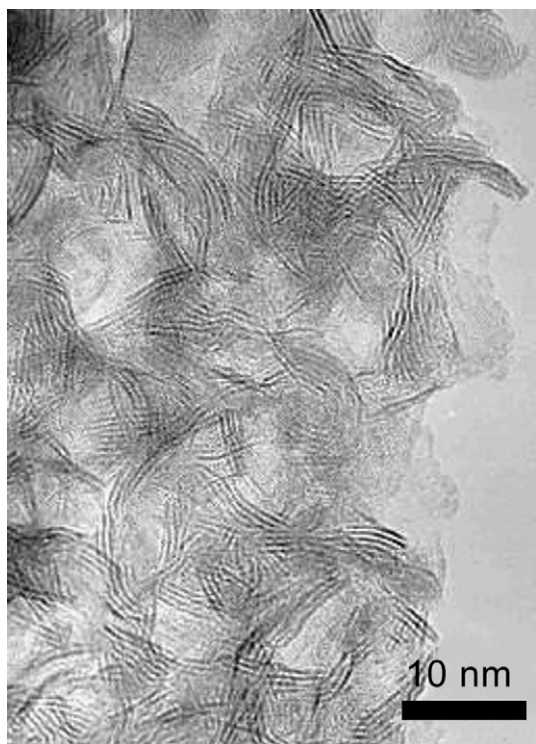


Fig. 5. HREM image of the Ni–W-450 catalyst.

- [30] G. Alonso, V. Petranovskii, M. Del Valle, J. Cruz-Reyes, A. Licea-Claverie, S. Fuentes, *Appl. Catal.*, A 197 (2000) 87.
- [31] G. Alonso, M.H. Siadati, G. Berhault, A. Aguilar, S. Fuentes, R.R. Chianelli, *Appl. Catal.*, A 263 (2004) 109.
- [32] G. Alonso, J. Espino, G. Berhault, L. Avarez, J.L. Rico, *Appl. Catal.*, A 266 (2004) 29.
- [33] D. Genuit, I. Bezverkhy, P. Afanasiev, *J. Solid State Chem.* 178 (2005) 2759.
- [34] D. Genuit, P. Afanasiev, M. Vrinat, *J. Catal.* 235 (2005) 302.
- [35] E. Payen, S. Kasztelan, J. Grimblot, J.P. Bonnelle, *Catal. Today* 4 (1988) 57.